Coherence Effects in Gaseous Lasers with Axial Magnetic Fields. I. Theoretical*

W. CULSHAW AND J. KANNELAUD
Lockheed Palo Alto Research Laboratory, Palo Alto, California
(Received 30 November 1964; revised manuscript received 15 July 1965)

The Lamb theory of the optical maser is applied to circularly polarized atomic transitions, and used to consider the beat frequencies and the coherence properties of such orthogonal fields when axial magnetic fields are applied to the gaseous laser. The beat frequency approaches zero in near-zero magnetic fields and synchronization can then occur between the right- and left-handed circularly polarized oscillations. For a resonator with no undue polarization constraint, such a strong coupling gives rise to a linearly polarized output, and to a rotation of the plane of polarization with increasing magnetic field. A self-consistent expression is derived for this rotation under steady-state conditions, and a maximum rotation of $\pm\frac{1}{4}\pi$ with magnetic field is indicated before the synchronization breaks down and circularly polarized beat phenomena appear. The rotation with magnetic field depends on the laser intensity, on the anisotropy in the cavity losses, and on the position of the cavity resonance within the Doppler linewidth. Also, the angle of rotation is indeterminate unless such anisotropy is present. Other regions of such coherence can occur at higher magnetic fields, where the beat frequency again approaches zero. These depend on the detailed shape of the various dispersion curves of the laser medium. The results derived from the theory used are in general agreement with experimental observations on the 1.153-μ He-Ne laser transition.

1. INTRODUCTION

EARLIER accounts of Zeeman studies[1,2] on gaseous lasers have discussed the beat-frequency phenomena due to independent laser oscillations in the distinct polarizations, or eigenstates, of the photon. In order to observe such low-frequency beats, as for example between separate laser oscillations in right- and left-handed circular polarizations, the axial magnetic field applied to the laser must be such that these oscillations are relatively independent. Each oscillation is then pulled towards the center of the respective line by frequency-pulling, or first-order dispersion effects, and also shifted in frequency by frequency-pushing, or power-dependent dispersion effects.[3] These dispersion effects lead to a frequency splitting of a given axial resonance of the laser cavity, and hence, account for the low-frequency beats.

These early investigations used long lasers, and the results were complicated by simultaneous oscillations in a number of axial modes. The results obtained on such lasers indicated that the beat frequency increased with magnetic field monotonically. More recent investigations on a short, single-mode laser,[4] have shown, however, that the beat frequency may reach a maximum value, depending on the laser intensity and tuning position within the Doppler linewidth and then decrease towards zero again as the magnetic field increases further. After passing through this additional region of zero beat frequency, the beat frequency again increases with magnetic field. Other regions of magnetic field in which the beat frequency approaches zero may also occur depending on conditions, and it is clear that at such values of magnetic field the Zeeman levels no longer overlap. It is, of course, necessary in such investigations that the Doppler linewidths of the transitions overlap, and that the laser be above threshold for both orthogonal polarizations.

In the region of zero magnetic field, where the Zeeman levels overlap, the beat frequency approaches zero and the dispersive effects are such that a single-laser frequency can act on both transitions, and make them phase coherent, or synchronous. A change in the polarization of the laser with increasing magnetic field may then be expected in this region owing to variations in the dispersive properties of the medium for the circular polarizations. The effect is similar to the well-known Hanle effect[5] in spontaneous emissive processes. However, similar changes may also occur around any other value of axial magnetic field for which the beat frequency again approaches zero. Here the dispersive effects in the medium are again equal for both polarizations and a single-laser frequency can operate on both transitions simultaneously. Such considerations allowed the prediction that a rotation of the plane of polarization of the output from a planar-type laser should occur when small axial magnetic fields are applied, and this was later confirmed experimentally on a short laser operating in a single mode.[4] In this work a dependence of the slope of the rotation versus magnetic field on the laser intensity was observed, and the existence of other regions of axial magnetic field giving zero beat frequency and a similar rotation was established.

Subsequently, the phenomenon has been investigated more precisely and additional experimental results on the variation of beat frequencies and on the dependence of the rotation of the polarization with axial magnetic field on the laser intensity, laser tuning, etc., have been obtained. These are dealt with in the experimental part

* Supported by the Lockheed Independent Research Funds.
[1] W. Culshaw and J. Kannelaud, Phys. Rev. **126**, 1747 (1962); **133**, A691 (1964).
[2] H. Statz, R. Paananen, and G. F. Koster, J. Appl. Phys. **33**, 2319 (1962); R. Paananen, C. L. Tang, and H. Statz, Proc. Inst. Elec. Electron. Engrs. **51**, 63 (1963).
[3] W. R. Bennett, Jr., Phys. Rev. **126**, 580 (1962).
[4] W. Culshaw and J. Kannelaud, Phys. Rev. **136**, A1209 (1964).
[5] W. Hanle, Z. Physik **30**, 93 (1924).

of the present account.[6] Here we apply the detailed theory of the optical maser, as given by Lamb,[7] to circularly polarized laser transitions, and deduce the expression for the beat frequency as a function of magnetic field. The existence of these other regions of zero beat frequency at specific values of magnetic field is thus shown, and examples are given. In these zero-beat regions the oscillations are locked together, and hence are combined coherently with appropriate phase differences. A self-consistent expression for the rotation of the polarization with magnetic field is thus derived. The theory explains the dependence of the rotation with magnetic field on the laser intensity, on the cavity tuning within the Doppler linewidth, and on the anisotropy in the cavity losses. The angle of rotation is indeterminate unless the Q values in orthogonal directions differ slightly. A maximum rotation of $\pm\frac{1}{4}\pi$ is predicted before the angle of rotation becomes indeterminate and circularly polarized beat phenomena appear. The value of magnetic field at which this occurs depends on the decay constants of the states involved, but is also dependent on the additional parameters considered here.

Such rotations of the plane of polarization at the specific values of magnetic field, where the frequencies of the orthogonal circularly polarized oscillations become the same, are due to a mutual synchronization of these otherwise relatively independent laser oscillations, and are very similar to the nonlinear effects encountered in the synchronization of other oscillatory phenomena.[8] Thus, the synchronization or locking of the frequency of a self-oscillatory system to the frequency of an injected signal is due to nonlinear effects in the oscillatory system, and the width of the frequency interval for which the oscillator has this same frequency is called the lock-in band. Similar frequency-locking effects have been observed between axial modes of the laser as the cavity tuning approaches the line center; these were initially observed by Javan and by Fork, and have also been discussed theoretically.[7,9] We are concerned here with similar effects in the region of zero beat frequency between the circularly polarized transitions. Here the nonlinearity is due to the response of the ensemble of atoms to the electric field within the laser cavity, and the coupling between the oscillations is strong in such regions. On leaving the lock-in band, the coupling becomes gradually weaker, until at a sufficiently higher value of magnetic field a single beat frequency between the circularly polarized oscillations appears. In the intermediate region, just outside any lock-in band, more complicated beat phenomena occur, presumably due to time-dependent phase relationships in the nonlinear coupling of these oscillations. These give rise to various numbers of harmonically related beat frequencies, which gradually reduce in number as the magnetic field increases. Such time-dependent coupling effects are complicated, and we shall not consider this intermediate region of magnetic field any further, although our results will give the width of the lock-in band.

2. CIRCULARLY POLARIZED TRANSITIONS

The $j=\frac{1}{2}\rightarrow j=\frac{1}{2}$ laser transition to be considered is shown in Fig. 1, in which certain values of magnetic field would give rise to independent circularly polarized oscillations and to a beat frequency varying with magnetic field. Other values of magnetic field will give zero beat frequency for some conditions of the laser and a single frequency can then operate on both transitions and couple them due to nonlinear effects in the medium. The results to be derived are strictly correct for the simple laser transition considered here, and any application of them to the more complicated $J=1\rightarrow J=2$ transition of the 1.153-μ He-Ne laser will require further consideration, and comparison with the experimental results. There are three σ_- and three σ_+ transitions involved in this more complicated system, which for unequal g values may lead to somewhat different results. However, if we assume the g values are comparable, say both around 1.3,[1,2] a normal Zeeman pattern would be obtained, and, as in our simple level scheme, only two atomic frequencies would be effective. In this event all the right-handed (r.h.) circularly polarized transitions would be made coherent by the single-laser frequency, which would also operate at the same position on the Doppler linewidth for all such transitions. Similar remarks apply for the left-handed (l.h.) circular polarized transitions, and the single beat frequency obtained would behave similarly to that for the simple four-level scheme. Some differences also occur because some of the $\Delta m=\pm 1$ transitions start or end on the same level in the He-Ne laser. However, provided no serious un-

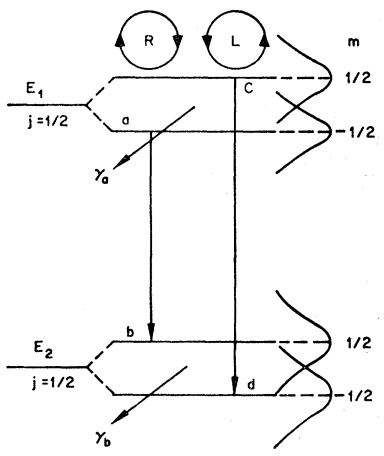

FIG. 1. Energy-level system and the transitions $\Delta m=\pm 1$ considered in the analysis of the beat frequencies and the rotation of polarization with magnetic field.

[6] J. Kannelaud and W. Culshaw, following paper, Phys. Rev. 141, 237 (1966).
[7] W. E. Lamb, Jr., Phys. Rev. 134, A1429 (1964).
[8] N. Minorsky, *Nonlinear Oscillations* (D. Van Nostrand Company, Inc., New York, 1962), pp. 438–459.
[9] C. L. Tang and H. Statz, Phys. Rev. 128, 1013 (1962).

balance occurs in the intensities of the orthogonal circularly polarized oscillations, which is a reasonable assumption at small magnetic fields, and is strictly correct when the cavity is initially tuned to the line center before the field is applied, the results derived with this much simpler level scheme should be applicable, at least as far as the general features are concerned, to this more complicated level scheme. A similar formulation of the problem could be done for these other level schemes, but is complicated by the multiplicity of transitions which are involved. In any event, phenomena similar to those derived from the approach used here are to be expected for all level schemes.

For laser oscillations in a single mode with r.h. circular polarization, the development of the electric field inside the laser cavity may be written in the form[7]

$$\mathbf{E}_n(z,t)=\tfrac{1}{2}E(t)[(\mathbf{i}-i\mathbf{j})e^{-i(\nu_n t+\phi_n)}+\text{c.c.}]\sin K_n z\,, \quad (1)$$

and the steady state of the laser oscillation is then determined from the real and imaginary parts of the conditional equation

$$\tfrac{1}{2}\mathbf{e}\left[-i\left(2\nu_n\dot{E}_n+\frac{\nu\nu_n}{Q_n}E_n\right)+E_n(\Omega_n^2-\nu_n^2)\right]e^{-i(\nu_n t+\phi_n)}+\text{c.c.}$$
$$=\frac{1}{2}\frac{\nu^2}{\epsilon_0}\mathbf{e}P_n(t)e^{-i(\nu_n t+\phi_n)}+\text{c.c.}, \quad (2)$$

where $\mathbf{e}$ is the polarization of the laser transition, $K_n=2\pi/L$, L is the cavity length, Ω_n is an eigenfrequency of the cavity without loss, and $P_n(t)$ is the macroscopic polarization, or source term, for laser oscillation at the frequency ν_n. The electric-dipole perturbation between levels a and b due to the laser emission is given by

$$\hbar\mathcal{H}_e=-e\mathbf{E}_r(z,t)\cdot\mathbf{r}\,, \quad (3)$$

and using Eq. (1), we require the quantum-mechanical average value of the electric-dipole operator

$$\Omega=e[(x-iy)+(x+iy)]\,, \quad (4)$$

for the particular atomic state concerned. This may be written as a linear superposition of states ψ_a and ψ_b

$$\psi(t)=a(t)\psi_a+b(t)\psi_b\,, \quad (5)$$

where the time dependence of the perturbation controls the time development of the coefficients $a(t)$ and $b(t)$, and hence the time development of the average value of the operator in Eq. (4). This may then be written

$$\langle\Omega\rangle=\text{tr}[\rho\Omega]\,, \quad (6)$$

where ρ is the density matrix of the two level scheme, from which the microscopic polarization is then given by

$$p(t)=\Delta^*a^*b+\Delta ab^*\,, \quad (7)$$

where $\Delta=e\Omega_{ba}$ is the matrix element of the operator Ω between states ψ_a and ψ_b.

The analysis now proceeds in the way developed by Lamb,[7] with the perturbation written as

$$\hbar V(t)=-\tfrac{1}{2}E_n[z+v(t-t_0),t]e^{-i(\nu_n t+\phi_n)}\,, \quad (8)$$

whence the equations of time-dependent perturbation theory become

$$\begin{aligned}i\dot{a}&=W_a a+V(t)b-\tfrac{1}{2}i\gamma_a a\,,\\ i\dot{b}&=W_b b+V^*(t)a-\tfrac{1}{2}i\gamma_b b\,,\end{aligned} \quad (9)$$

where $\hbar W_a$ and $\hbar W_b$ represent the energies of states a and b in angular frequency units. The expression for the macroscopic polarization, or source term for the r.h. circularly polarized oscillation may then to first order in the perturbation V be written as

$$P_n{}^{r(1)}(t)=-\tfrac{1}{2}C_1\mathbf{e}_r E_n(t)\bar{N}Z(\nu_n-\omega_r)e^{-i(\nu_n t+\phi_n)}+\text{c.c.}, \quad (10)$$

where $C_1=|\Delta|^2/\hbar ku$, $\mathbf{e}_r$ is equal to $\mathbf{i}-i\mathbf{j}$, and represents the vector nature of the photon involved in the transition. $Z(\nu_n-\omega_r)$ is the complex dispersion function of the assumed Maxwellian velocity distribution,[7,10] ku is the Doppler width parameter, and ω_r is the atomic frequency of the r.h. circularly polarized transition. $\bar{N}$ is the mean value of the excitation density for a single mode of oscillation. Substituting the value of $P_n(t)$ from Eq. (10) into Eq. (2), gives the equations which determine the threshold for oscillation, and also the frequency-pulling effects due to the dispersive properties of the medium.

Similarly the third-order term in the macroscopic polarization for a single mode is given by[7]

$$P_n{}^{r(3)}(t)=\tfrac{1}{16}C_2\mathbf{e}_r E_n{}^3\bar{N}(P_r{}^r+iP_i{}^r)e^{-i(\nu_n t+\phi_n)}+\text{c.c.}, \quad (11)$$

where $C_2=\pi^{1/2}|\Delta|^4/\hbar^3\gamma_a\gamma_b ku$, and where

$$P_r{}^r=\gamma_{ab}(\omega_r-\nu_n)\mathfrak{L}(\omega_r-\nu_n)\,, \quad (12)$$

$$P_i{}^r=1+\gamma_{ab}{}^2\mathfrak{L}(\omega_r-\nu_n)\,, \quad (13)$$

with $\gamma_{ab}=\tfrac{1}{2}(\gamma_a+\gamma_b)$, denote the real and imaginary parts of the third-order dispersion function P^r. The steady state of this oscillation is now determined from Eqs. (2), (10), and (11), and the total frequency shift of the oscillation due to both frequency pulling and pushing effects is then given by

$$\nu_n{}^r=\Omega_n+\tfrac{1}{2}(\nu/Q)\left[\eta\frac{Z_r(\Omega_n-\omega_r)}{Z_i(0)}-\left(\frac{Z_i(\Omega_n-\omega_r)}{Z_i(0)}\eta-1\right)\frac{P_r{}^r}{P_i{}^r}\right], \quad (14)$$

where Z_r and Z_i are the real and imaginary parts of $Z(\nu_n-\omega_r)$, and the frequency ν_n in the dispersion functions $P_r{}^r$ and $P_i{}^r$ is replaced by Ω_n, to a good approxima-

[10] B. D. Fried and S. D. Conte, *The Plasma Dispersion Function Hilbert Transform of the Gaussian* (Academic Press Inc., New York, 1961).

tion. η is the relative excitation given by

$$\eta=\bar{N}/\bar{N}_t, \tag{15}$$

where

$$\bar{N}_t=\epsilon_0/C_1Z_i(0)Q \tag{16}$$

is the threshold excitation density when the laser is tuned to the line center.

Analogous results may be written down for the l.h. circularly polarized transition $c\rightarrow d$ in Fig. 1. Thus, the first- and third-order macroscopic polarization terms are given by

$$P_n{}^{l(1)}(t)=-\tfrac{1}{2}C_1\mathbf{e}_lE_n(t)\bar{N}Z(\nu_n-\omega_l)e^{-i(\nu_nt+\phi_n)}+\text{c.c.}, \tag{17}$$

$$P_n{}^{l(3)}(t)=\tfrac{1}{16}C_2\mathbf{e}_lE_n{}^3\bar{N}(P_r{}^l+iP_i{}^l)e^{-i(\nu_nt+\phi_n)}, \tag{18}$$

respectively, where the frequency and phase angles may of course be different from those of the r.h. circularly polarization, and $\mathbf{e}_l=\mathbf{i}+i\mathbf{j}$. An equation for the frequency $\nu_n{}^l$ then follows by substituting ω_l, the frequency of the l.h. circularly polarized transition, into Eqs. (12), (13), and (14). The excitation parameter η is the same for both transitions.

3. BEAT FREQUENCIES

Using Eq. (14) for r.h. and its counterpart for l.h. circularly polarized radiation, the beat frequency, which will be observed on detecting these radiations with an analyzer and photomultiplier, may be written as

$$\begin{aligned}\nu_n{}^r-\nu_n{}^l=\frac{1}{2}\left(\frac{\nu}{Q}\right)\Bigg\{&\frac{\eta}{Z_i(0)}[Z_r(\Omega_n-\omega_r)-Z_r(\Omega_n-\omega_l)]\\&-\left[\frac{Z_i(\Omega_n-\omega_r)}{Z_i(0)}\eta-1\right]\frac{P_r{}^r}{P_i{}^r}\\&+\left[\frac{Z_i(\Omega_n-\omega_l)}{Z_i(0)}\eta-1\right]\frac{P_r{}^l}{P_i{}^l}\Bigg\}.\end{aligned} \tag{19}$$

It is clear from Eq. (19) that both first-order dispersion effects (frequency-pulling), and third-order (frequency-pushing) effects will be effective in determining the beat frequency. This will thus depend on the detailed shape of the first- and third-order dispersions functions involved, and also on the laser intensity, and on the Q value of the laser cavity. The functions $Z_r(\omega)$ and $Z_i(\omega)$ are shown in Fig. 2 for a Doppler parameter ku equivalent to 500 Mc/sec, and for values of γ_{ab}/ku equal to zero and 0.1, respectively. Similarly, the third-order dispersion functions are shown in Fig. 3 for values of $\gamma_{ab}/2\pi$ of 20 Mc/sec and 50 Mc/sec, respectively. The operating point on these curves, and thus the beat-frequency variation with magnetic field, is determined by the deviation of the cavity frequency from the line center, or by $\Omega_n-\omega$, where ω is the atomic frequency in the absence of magnetic fields. There will thus be marked variations in the beat frequency with cavity tuning, and while the beat frequency is zero in zero magnetic field, it may also become zero again at a higher value of magnetic field, particularly in the vicinity of the stationary points of the dispersion curves $Z_r(\omega)$ and $P_r(\omega)$. The symmetry relations $Z_r(\omega)=-Z_r(-\omega)$, $Z_i(\omega)=Z_i(-\omega)$, $P_r(\omega)=-P_r(-\omega)$, $P_i(\omega)=P_i(-\omega)$ should be noted, and also that $Z_r(\omega)$ is negative and $P_r(\omega)$ is positive for positive ω.

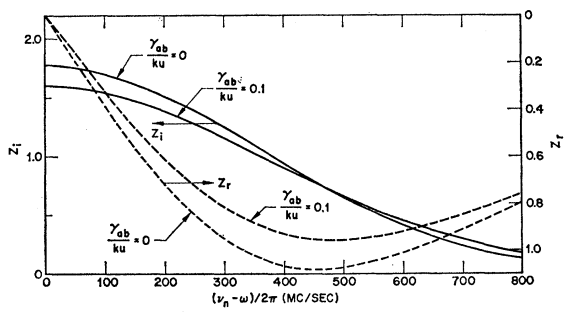

FIG. 2. Graphs of the real and imaginary parts, Z_r and Z_i of the first-order dispersion function $Z(\nu_n-\omega)$.

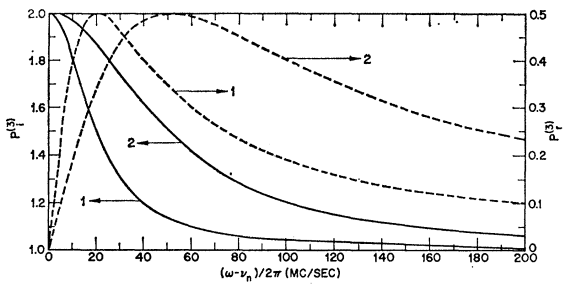

FIG. 3. Graphs of the real and imaginary parts P_r and P_i of the third-order polarization term $P(\omega)$. The parameter γ_{ab} is equal to $4\pi\times10^7$ and $10\pi\times10^7$ sec^{-1} for curves 1 and 2, respectively.

Assuming that $\nu/Q=10^6$, and $\gamma_{ab}/ku=0$, Fig. 4 shows plots of the beat frequency $\nu_n{}^r-\nu_n{}^l$ against the Zeeman shift $(\omega-\omega_r)$ or $(\omega_l-\omega)$, for $\eta=2$ and 1.2 and for $\gamma_{ab}/2\pi=20$ and 50 Mc/sec, respectively. The laser cavity is initially tuned to the line center, or $\Omega_n-\omega$ is zero, when Eq. (19) reduces to the form

$$\nu_n{}^r-\nu_n{}^l=\frac{\nu}{Q}\left[\eta\frac{Z_r{}^r}{Z_i(0)}-\left(\frac{Z_i{}^r}{Z_i(0)}\eta-1\right)\frac{P_r{}^r}{P_i{}^r}\right], \tag{20}$$

where the superscript r indicates that the functions refer to a r.h. circularly polarized transition. Referring to curve 1, for $\eta=2$ and $\gamma_{ab}/2\pi=20$ Mc/sec, we see that as the magnetic field increases from zero the beat frequency is positive, showing that frequency-pushing effects are dominant for these parameters. This is due to the more rapid increase in the function $P_r(\omega)$ of Fig. 3, as compared with the function $Z_r(\omega)$ shown in Fig. 2. The beat frequency, thus, attains a maximum of some $+240$ kc/sec at a magnetic field corresponding to $(\omega-\omega_r)/2\pi=\Delta f_H=22$ Mc/sec, when the frequency-

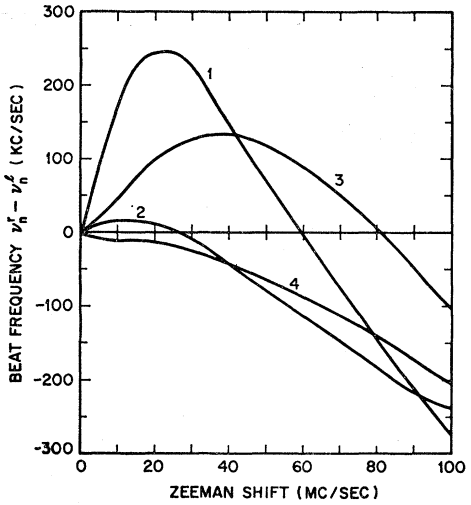

FIG. 4. Variation of beat frequency with $\omega-\omega_r$, the Zeeman shift. Cavity tuned to line center initially. Curve 1, $\eta=2$, $\gamma_{ab}/2\pi=20$. Curve 2, $\eta=1.2$, $\gamma_{ab}/2\pi=20$. Curve 3, $\eta=2$, $\gamma_{ab}/2\pi=50$. Curve 4, $\eta=1.2$, $\gamma_{ab}/2\pi=50$. All frequencies expressed in Mc/sec.

pushing effects start to decrease again as shown in Fig. 3. The beat frequency passes through zero at a magnetic field corresponding to Δf_H equal to some 60 Mc/sec, and then the beat frequency becomes negative and decreases with increasing magnetic field due to the function $Z_r(\omega)$ in the normal way. Curve 2 exhibits the same behavior modified only by the lower value of $\eta=1.2$. Curves 3 and 4 apply for the large value of $\gamma_{ab}/2\pi=50$ Mc/sec; the second zero-beat region for $\eta=2$, then occurs at the higher value of 80 Mc/sec, while in Curve 4, for $\eta=1.2$, a positive beat frequency is never attained and no other region of zero beat frequency occurs.

Figure 5 shows similar curves deduced from Eq. (19) for various values of $(\Omega_n-\omega)/2\pi=\Delta f$, the tuning of the laser cavity with respect to the line center. Here $\gamma_{ab}/2\pi=20$ Mc/sec, and $\eta=5$ for all curves, which corresponds to operation well above threshold at the line center. For curve 1, $\Delta f=50$ Mc/sec and the beat frequency is initially negative since both $Z_r(\omega)$ and $P_r(\omega)$ are negative and $|P_r{}^l(\omega)|>|P_r{}^r(\omega)|$. After the frequency Δf_H increases so that $P_r(\omega)$ passes through the optimum value shown in Fig. 3, the beat frequency starts to increase and passes through zero at $\Delta f_H=59$ Mc/sec. The beat frequency then becomes positive and increases to a value of +200 kc/sec. Frequency-pushing effects then start to decrease, and the beat frequency passes through zero again at $\Delta f_H=85$ Mc/sec becoming negative due to the usual frequency-pulling effects of the function $Z_r(\omega)$. Curve 2 for $\Delta f=100$ Mc/sec exhibits a similar behavior due to the resonance in the $P_r(\omega)$ curve of Fig. 3, but never becomes positive, due to the larger value of Δf, Curve 3 for $\Delta f=300$ Mc/sec corresponds to operation well down the curves of $P_r(\omega)$ and $P_i(\omega)$ and the resonance position is never attained for the values of Zeeman shifts Δf_H used here. The beat frequency is thus negative and decreases steadily due essentially to frequency-pulling effects. Curve 4 for $\Delta f=500$ Mc/sec corresponds to operation around the stationary points of the dispersion function $Z_r(\omega)$, and the effects of the frequency-pushing terms $P_r(\omega)$ are then very small. The beat frequencies are then also small since $Z_r{}^r(\omega)\approx Z_r{}^l(\omega)$, and for the case shown they are positive because $Z_r(\omega)>Z_l(\omega)$. The beat frequency would pass through zero at some higher value of Δf_H and for a larger value of η, corresponding to some position around the stationary point at which $Z_r{}^r(\omega)=Z_r{}^l(\omega)$.[11] It is apparent that these somewhat anomalous results for the beat-frequency variation with magnetic field are associated with the third-order dispersion functions $P(\omega)$ as defined by Eqs. (12) and (13), and in particular with the resonance in the real part of this function at $\Delta f_H=\gamma_{ab}/2\pi$.

4. COHERENT COMBINATION OF THE CIRCULAR POLARIZATIONS

We see from Figs. 4 and 5 that the beat frequency between the orthogonal circularly polarized modes is zero for zero magnetic field, and also for other finite values of magnetic field which depend on the particular operating conditions. When the magnetic field is such that a zero beat frequency occurs, the dispersive effects

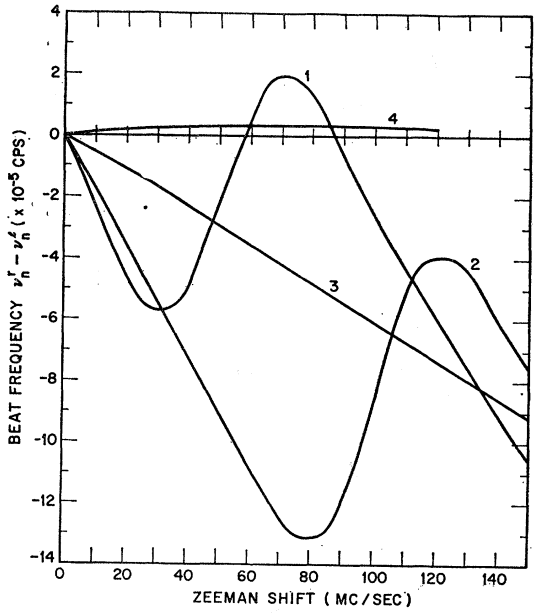

FIG. 5. Variation of beat frequency with $\omega-\omega_r=\omega_l=\omega=\Delta f_H$, the Zeeman shift and with cavity tuning position Δf on the Doppler linewidth. Curve 1, $\Delta f=50$. Curve 2, $\Delta f=100$. Curve 3, $\Delta f=300$. Curve 4, $\Delta f=500$. $\eta=5$, $\gamma_{ab}/2\pi=20$ for all curves. All frequencies expressed in Mc/sec.

[11] Similar beat-frequency curves for first-order dispersion, or frequency-pulling effects, have been given by A. Corney [(private communication), and Phys. Letters (to be published)].

of the laser medium are identical for both photon types, and a single-laser frequency will tend to synchronize, or couple both circularly polarized transitions $\Delta m=\pm 1$ together due to the nonlinear properties of the medium. The range of magnetic field over which this coupling or coherence persists will depend on the dispersive properties of the medium for the respective polarizations, and we may expect that, while a single laser frequency acts on both transitions, there will, however, be a varying phase relationship between the two oscillations which depends on the magnetic field. This will enable us to explain the observed linear polarization in zero magnetic field, and in other regions of zero beat frequency, and also the rotation of the plane of polarization which is observed as the magnetic field is varied around such regions.[4,6]

Accordingly, to obtain a laser oscillation with the electric vector linearly polarized at some angle ϕ to the x axis as in Fig. 6, the corresponding circularly polarized waves are written in the form

$$\begin{aligned} E_n(z,t)&=\tfrac{1}{4}E_n(t)[\mathbf{e}_r e^{-i(\nu_n t-\phi)}+\text{c.c.}]U_n(z)\,,\\ E_n(z,t)&=\tfrac{1}{4}E_n(t)[\mathbf{e}_l e^{-i(\nu_n t+\phi)}+\text{c.c.}]U_n(z)\,, \end{aligned} \tag{21}$$

which gives the components of electric field

$$\begin{aligned} E_x(t)&=E_n(t)\,\cos\nu_n t\,\cos\phi\,,\\ E_y(t)&=E_n(t)\,\cos\nu_n t\,\sin\phi\,. \end{aligned} \tag{22}$$

Here the x direction may be taken as the direction of polarization in zero magnetic field. The self-consistent equations for the x direction may now be written as[7]

$$\begin{aligned} (\nu_n-\Omega_n)E_n\cos\phi&=-\tfrac{1}{2}(\nu/\epsilon_0)C_n(\phi,t)\,,\\ [\dot{E}_n+\tfrac{1}{2}(\nu/Q_n)E_n]\cos\phi&=-\tfrac{1}{2}(\nu/\epsilon_0)S_n(\phi,t)\,, \end{aligned} \tag{23}$$

with similar equations involving $\sin\phi$ for the y direction. Here the macroscopic polarization has been expressed in the form

$$\begin{aligned} \mathbf{P}_n(\phi,t)=\mathbf{i}[&C_n(\phi,t)\,\cos\nu_n t+S_n(\phi,t)\,\sin\nu_n t]\\ &+\mathbf{j}[C_n'(\phi,t)\,\cos\nu_n t+S_n'(\phi,t)\,\sin\nu_n t]\,. \end{aligned} \tag{24}$$

With appropriate changes in the numerical constant, Eqs. (10) and (17), are now added, because of the strong coupling in the region under consideration, to obtain the resultant first-order polarization along the x and y directions, with the results

$$\begin{aligned} P_x^{(1)}(t)=-\tfrac{1}{2}C_1E_n(t)\bar{N}[&(Y'\cos\phi-X'\sin\phi)\,\cos\nu_n t\\ &+(X\cos\phi+Y\sin\phi)\,\sin\nu_n t]\,, \end{aligned} \tag{25}$$

$$\begin{aligned} P_y^{(1)}(t)=-\tfrac{1}{2}C_1E_n(t)\bar{N}[&(X'\cos\phi+Y'\sin\phi)\,\cos\nu_n t\\ &-(Y\cos\phi-X\sin\phi)\,\sin\nu_n t]\,, \end{aligned} \tag{26}$$

where

$$\begin{aligned} X&=Z_i^r+Z_i^l\,,\quad X'=Z_i^r-Z_i^l\,,\\ Y&=Z_r^r-Z_r^l\,,\quad Y'=Z_r^r+Z_r^l\,. \end{aligned} \tag{27}$$

When the laser is tuned to the line center before the magnetic field is applied, we have $Z_i^r=Z_i^l$, and $Z_r^r=-Z_r^l$, and Eqs. (25) and (26) reduce to the form

$$P_x^{(1)}(t)=-C_1E_n(t)\bar{N}(Z_i^r\cos\phi+Z_r^r\sin\phi)\,\sin\nu_n t\,, \tag{28}$$

$$P_y^{(1)}(t)=-C_1E_n(t)\bar{N}(-Z_r^r\cos\phi+Z_i^r\sin\phi)\,\sin\nu_n t\,, \tag{29}$$

and all terms in $\cos\nu_n t$ are zero, which by comparison with Eqs. (23) and (24) shows that there are no frequency-pulling effects in this case. The threshold relations for the x and y direstions, corresponding to $\phi=0$, and $\phi=\frac{1}{2}\pi$, respectively, in Eqs. (28) and (29) for zero magnetic field, are then given by

$$Q_x^{-1}=C_1\bar{N}_x{}^tZ_i(0)\,,\quad Q_y^{-1}=C_1\bar{N}_y{}^tZ_i(0)\,, \tag{30}$$

where, for reasons which will appear later, we assume that the values Q_x and Q_y differ slightly. The relative excitation parameters may then be written as

$$\eta_x=\bar{N}/\bar{N}_x{}^t\,,\quad \eta_y=\bar{N}/\bar{N}_y{}^t\,. \tag{31}$$

Similarly, the third-order polarizations given by Eqs. (11) and (18) are combined to give the results

$$\begin{aligned} P_x^{(3)}(t)=\tfrac{1}{64}C_2E_n{}^3(t)[&(y'\cos\phi-x'\sin\phi)\,\cos\nu_n t\\ &+(x\cos\phi+y\sin\phi)\,\sin\nu_n t]\,, \end{aligned} \tag{32}$$

$$\begin{aligned} P_y^{(3)}(t)=\tfrac{1}{64}C_2E_n{}^3(t)[&(x'\cos\phi+y'\sin\phi)\,\cos\nu_n t\\ &-(y\cos\phi-x\sin\phi)\,\sin\nu_n t]\,, \end{aligned} \tag{33}$$

where

$$\begin{aligned} x&=P_i{}^r+P_i{}^l\,,\quad x'=P_i{}^r-P_i{}^l\,,\\ y&=P_r{}^r-P_r{}^l\,,\quad y'=P_r{}^r+P_r{}^l\,. \end{aligned} \tag{34}$$

These equations, together with Eqs. (23), (24), (25), and (26), will determine the steady-state conditions in the x and y directions. We note that when the cavity is tuned to the line center $P_r{}^r=-P_r{}^l$ and $P_i{}^r=P_i{}^l$, and the terms involving $\cos\nu_n t$ in Eqs. (32) and (33) become zero and there are then no frequency pushing effects.

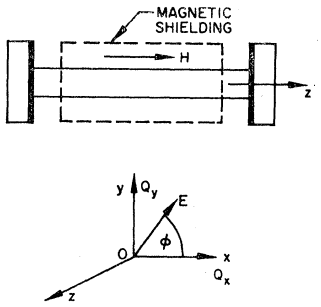

FIG. 6. Coordinate system used in the analysis with an axial magnetic field, and the laser radiation polarized at some angle ϕ to the x axis.

5. EQUATION OF CONSISTENCY FOR THE ANGLE ϕ

We have considered in Sec. 3 a specific region of magnetic field in which the orthogonal circularly polarized transitions are coupled together by a single-laser frequency, and we have combined the macroscopic polarizations along the x and y directions. The angle of the

assumed linearly polarized laser output is now determined from the equations which govern the steady-state oscillations in these directions, and by determining the ratio of these component field intensities as a function of ϕ. The relation

$$E_y^2/E_x^2=\tan^2\phi \tag{35}$$

must then hold for consistency, and this leads to an equation for $\tan\phi$.

The steady-state components of the oscillation along the x and y directions are determined by equations of the form

$$\begin{aligned}\dot{E}_x&=\alpha_i E_x-\beta_i E_x^3,\\ \dot{E}_y&=\alpha_j E_y-\beta_j E_y^3,\end{aligned} \tag{36}$$

from which we obtain for the steady state the relation

$$E_y^2/E_x^2=\alpha_j\beta_i/\alpha_i\beta_j=\tan^2\phi. \tag{37}$$

From Eqs. (23) through (33), we find that

$$\begin{aligned}\alpha_i&=(\nu/2)[-Q_x^{-1}+\epsilon_0^{-1}C_1\bar{N}\\ &\quad\times(X\cos\phi+Y\sin\phi)(\cos\phi)^{-1}],\\ \beta_i&=\tfrac{1}{64}(\nu/\epsilon_0)C_2\bar{N}(x\cos\phi+y\sin\phi)(\cos\phi)^{-3},\end{aligned} \tag{38}$$

and

$$\begin{aligned}\alpha_j&=(\nu/2)[-Q_y^{-1}+\epsilon_0^{-1}C_1\bar{N}\\ &\quad\times(-Y\cos\phi+X\sin\phi)(\sin\phi)^{-1}],\\ \beta_j&=\tfrac{1}{64}(\nu/\epsilon_0)C_2\bar{N}(-y\cos\phi+x\sin\phi)(\sin\phi)^{-3},\end{aligned} \tag{39}$$

since $E_x=E_n\cos\varphi$, $E_y=E_n\sin\phi$. The substitution of these results into Eq. (37) leads to the equation which must be satisfied by ϕ, and after some reduction we obtain the result

$$\tan\phi=[-b\pm(b^2-4ac)^{1/2}](2a)^{-1}, \tag{40}$$

where

$$\begin{aligned}a&=Xy-\eta_r Yx-ry\eta_y^{-1},\\ c&=\eta_r Xy-Yx-ry\eta_y^{-1},\\ b&=Xx(1-\eta_r)+Yy(\eta_r-1),\\ r&=2Z_i(0),\end{aligned} \tag{41}$$

with the parameters η_x and η_y determined by Eq. (31), and where we write

$$\eta_r=\eta_x/\eta_y. \tag{42}$$

Thus plus or minus sign in front of the radical in Eq. (40) refers to $\phi=\frac{1}{2}\pi$ and zero, respectively, in zero magnetic field, and we take the minus sign. The angle ϕ will thus be zero in zero magnetic field and will either increase or decrease as this field increases from zero, depending on the sign of the parameter a. Similar effects and a rotation of the plane of polarization will occur around any other position of zero beat frequency. Thus, $|\phi|$ will increase with magnetic field until $4ac>b^2$ at which field $\tan\phi$ becomes complex and the transition region between the linearly polarized output and the separate circularly polarized oscillations occurs. At this point $b\approx 2a$, and from Eq. (40) we see that rotations around $\frac{1}{4}\pi$ are indicated. In the unlikely case that $Q_x=Q_y$ we see that $a=c$ and hence $\tan\phi=\pm i$, and is thus indeterminate. Hence, in order to observe the phenomena, the Q value of the laser cavity must be anisotropic, and the actual rotation observed for a given value of magnetic field will depend on the degree to which this occurs. From the expression for b we deduce that the slope of the rotation with magnetic field will increase as $\eta_r\to 1$, or as Q_x and Q_y approach equality. It is apparent that such effects are due to a mutual synchronization of the circular polarizations due to the nonlinear properties of the ensemble of atoms within the cavity[1] and which will occur in any region of axial magnetic field for which the beat frequency tends to zero. The region of magnetic field in the vicinity of the zero beat in which the linear polarization and rotation occurs may be related to the lock-in bandwidth for the various operating conditions.

We also see from Eq. (40) that the slope of the rotation with magnetic field will change sign each time a passes through zero. The additional regions of coherence, or mutual synchronization, between such oscillations are thus, also determined by the values of magnetic field at which the parameter a, given by Eq. (41), is zero, which leads to the expression

$$\eta\frac{Z_r^r}{Z_i(0)}-\left(\frac{Z_i^r}{Z_i(0)}\eta-1\right)\frac{P_r^r}{P_i^r}=0, \tag{43}$$

if the laser is tuned to the line center, and we put $\eta_r=1$, and $\eta_y=\eta$. Equation (43) is then identical with the equation for zero beat frequency as deduced from Eq. (20), and again shows the close connection between the regions of the rotation of polarization and the region of zero beat frequency. Similar comparisons between the regions of magnetic field at which the beat frequency $\Delta\nu$ approaches zero, and those corresponding to a equal to zero, may be made for various cavity tuning positions using Eqs. (19) and (41). Thus, referring to Fig. 5, Curve 1 we see that $\Delta\nu$ is zero at Zeeman shifts Δf_H of 55.25 and at 88.3 Mc/sec. From Eq. (41) we find that $a=0$ for the same parameters, when $\Delta f_H=55.9$ and 89 Mc/sec, if we take $\eta_r=1.0$. For other values of η_r around unity these values will change, but the agreement is reasonable, and serves as check on the formulation since the value $a=0$ must lie within the lock-in region.

Resolving the polarizations given by Eqs. (25), (26), (32), and (33) along the direction of the resultant field $E_n(t)$, and using similar equations derived from Eq. (23), we find that the frequency shift and steady-state intensity of the coupled oscillation are given by

$$\nu_n=\Omega_n+\frac{1}{4}\frac{\nu}{Q}\left[\eta\frac{Y'}{Z_i(0)}-\left(\eta\frac{X}{Z_i(0)}-2\right)\frac{y'}{x}\right], \tag{44}$$

$$\frac{E_n^2|\Delta|^2}{\hbar^2\gamma_a\gamma_b}=\frac{32[X/Z_i(0)-2\eta^{-1}]}{x}, \tag{45}$$

where the threshold excitation is again defined by Eqs. (15) and (16). Thus, for an asymmetric tuning of the cavity with respect to the Doppler linewidth, there will be slight changes in the frequency and intensity as the magnetic field varies within the lock-in regions.

Figure 7 shows some computed results for the rotation of the polarization of the laser output as the axial magnetic field increases from zero. These have been deduced from Eq. (40) for the laser tuned to the line center, or $\Delta f=0$, and with $\gamma_{ab}/2\pi=20$ Mc/sec. The values $\eta_r=1.01$, and 1.001 with $\eta_y=1$ and 2 were used as indicated in the various curves. The following characteristics of the rotation are apparent: (a) For a fixed level of laser intensity, the slope of the rotation with magnetic field is greater the closer η_r is to unity; (b) the slope of the rotation with magnetic field increases with laser intensity; (c) for a fixed value of η_r the slope of the curves should change sign as η_y decreases towards

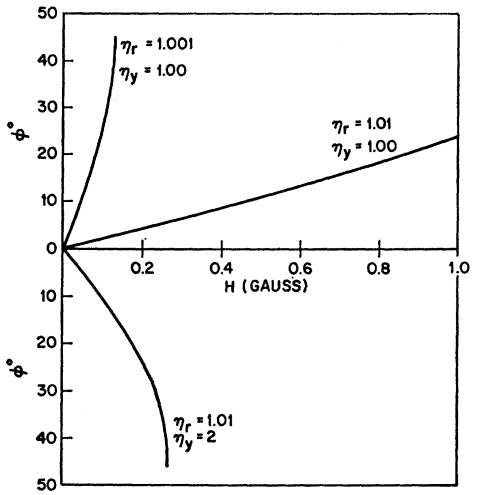

FIG. 7. Theoretical curves of rotation of polarization versus axial magnetic field for cavity resonance centered on the Doppler linewidth. Note the increased rate of rotation with laser intensity, and also as the Q values tend to equality, or $\eta_r \to 1$.

threshold; and (d) axial magnetic fields of a few tenths of a gauss should produce rotations around $\frac{1}{4}\pi$.

Figures 8 and 9 show similar curves for various frequency deviations Δf of the tuning from the line center. Here the values $\gamma_{ab}/2\pi=20$ and 50 Mc/sec were used in the respective figures, together with the indicated values of η_r and η_y. From these results it is apparent that (a) the slope of the curves increases with laser intensity; (b) the slope changes from negative to position in the region that Δf approaches $\gamma_{ab}/2\pi$; (c) the slope of the curves is a maximum for all η_y, η_r when the laser is tuned to the line center, at least for the values of $\gamma_{ab}/2\pi$ considered here; and (d) the slope is smaller for the larger value of γ_{ab}. A Zeeman shift of 1.8 Mc/sec/G was assumed in these computations, corresponding to the approximate value for the 1.153-μ He-Ne laser transition.

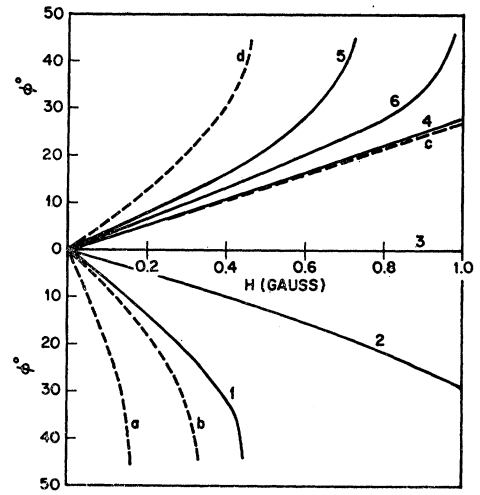

FIG. 8. Theoretical curves of the rotation of polarization versus magnetic field for frequency deviations $\Delta f=(\nu_n-\omega)/2\pi$ Mc/sec of the cavity tuning from the Doppler line center. Full curves: No. 1, $\Delta f=0$; No. 2, $\Delta f=10$; No. 3, $\Delta f=14.1$; No. 4, $\Delta f=20$; No. 5, $\Delta f=50$; No. 6, $\Delta f=100$. $\eta_y=1.5$ for all curves. Dashed curves: a, $\Delta f=0$; b, $\Delta f=10$, c, $\Delta f=20$; d, $\Delta f=50$. $\eta_y=5.0$. $\eta_r=1.01$, and $\gamma_{ab}=4\pi\times10^7$ sec^{-1} for all curves.

6. CONCLUSIONS

We have considered a relatively simple four-level laser transition giving circularly polarized beat phenomena when axial magnetic fields are applied. The appearance of a single beat frequency in such cases represents a steady state of the system in the limit of very small coupling between the oscillations. However, the frequency-pulling and -pushing effects at specific values of magnetic field may become identical for these two modes of opposite circular polarization, and hence the beat frequency may approach zero. In such regions,

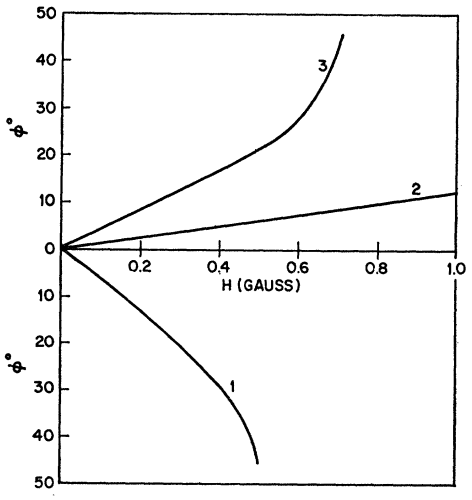

FIG. 9. Theoretical curves of the rotation of polarization versus magnetic field for frequency deviations Δf in Mc/sec from the line center. $\gamma_{ab}=10\pi\times10^7$ sec^{-1}. No. 1, $\Delta f=0$; No. 2, $\Delta f=50$; No. 3, $\Delta f=100$. $\eta_y=5$, $\eta_r=1.01$ for all curves.

the two frequencies have a natural tendency to coalesce due to the nonlinear effects in the interaction of the atomic system with the electromagnetic field inside the cavity. A coherence or mutual synchronization of the circularly polarized oscillations then occurs, giving rise to lock-in regions of the magnetic field in which only a single frequency is present. The polarization then becomes linear due to a strong coupling of the oscillations, and the plane of polarization rotates throughout the lock-in region due to a changing phase relationship between the two oscillations. A maximum rotation of $\pm\frac{1}{4}\pi$ is indicated before the strong coupling breaks down and circularly polarized modulation phenomena appear. Such a maximum rotation corresponds to a maximum phase difference of $\frac{1}{2}\pi$ between the oscillations, and would correspond to the similar phase condition which is applicable in the synchronization of an oscillator by an external signal.[12] Such coupling effects will occur in any region of magnetic field in which the beat frequency tends to zero and can be used to study the dispersive properties of the laser medium and the atomic parameters and collisional effects which are involved. The region of intermediate, or quasicoupling between the oscillations is more complicated and has not been considered in detail. Such a region will probably give rise to transient or modulation effects corresponding to harmonically related beat frequencies, which will give rise to a single beat frequency as the magnetic increases beyond this region.

The general implications of the theory, although strictly valid only for the particular transition considered, are, however, in agreement with previous observations[4] on the rotation of polarization with magnetic field of the more complicated 1.153-μ He-Ne laser transition. They also agree with the more detailed experimental investigations on this transition which are described in Part II.[6] Thus, the dependence of the rotation on the laser intensity, on the cavity tuning within the Doppler linewidth, and on the anisotropy of the cavity losses are all correctly predicted. The occurrence of additional regions of coherence at higher values of magnetic field and different cavity tuning positions is given by the Zeeman shifts at which the parameter a passes through zero. The positions thus derived are in good agreement with those deduced from considerations of the regions in which the beat frequency approaches zero. A change in sign of the slope of the rotation with magnetic field in alternate coherence regions is also indicated by the theory. As intimated in Sec. 2, similar phenomenon may be expected for any other laser transition in an axial magnetic field. Here we have been concerned with the general features of the effect, and not with any quantitative comparison with observations on a more complicated laser transition. Complications would in any event arise is a detailed comparison because of the lack of knowledge of all the parameters involved. However, further precise experimental investigations may well require that the actual transition involved must be considered in a similar, but more complicated way.[13]

[12] A. A. Kharkevich, *Nonlinear and Parametric Phenomena in Radio Engineering* (John F. Rider Publisher, Inc., New York, 1962), pp. 128–156.

[13] *Note added in proof.* Equations describing the beat-frequency variation and mode competition in a gaseous laser with an axial magnetic field have recently been given by Fork and Sargent, for the $J=1\rightarrow 0$ transition. [See R. L. Fork and M. Sargent, III, Phys. Rev. **139**, A617 (1965).]